Preprints of the 18th IFAC World Congress
Milano (Italy) August 28 - September 2, 2011

# Terminal Sliding Mode Control of a Twin Rotor Multiple-Input Multiple-Output System

**Anup K. Ekbote** * **N. S. Srinivasan** * **Arun D. Mahindrakar** *

* *Department of Electrical Engineering, Indian Institute of Technology Madras, Chennai - 600036, India* (e-mail: anupekbote@gmail.com, srinivasan.id@gmail.com, arun_dm@iitm.ac.in)

**Abstract:** This paper deals with the finite time stabilization of a twin rotor multiple-input multiple-output (TRMS) system. A terminal sliding mode control law is obtained for the linearized model of the system by transforming it to the Brunovsky canonical form. Through experiment, the resulting control law is shown to be stable to disturbances in pitch and yaw.

*Keywords:* Terminal sliding-mode control, Dynamic modelling, Non-minimum phase systems, Twin rotor, State space

## 1. INTRODUCTION

The twin rotor multiple-input multiple-output system, as shown in Figure 1, is a mechanical system with two links, a horizontal link connected to the base through a rotational joint and a link perpendicular to the horizontal link connected through another rotational joint with propellers attached at both ends. Vertical motion of the system is primarily influenced by the main rotor and horizontal motion is primarily influenced by the tail rotor. Both these rotors are driven by DC motors, enabling change of speed.

A mathematical modeling of the TRMS is presented in Rahideh and Shaheed (2007) based on Newtonian and Lagrangian methods. The modeling is carried out by considering the motor dynamics separately, thereby not considering the reaction due the main propeller and tail propeller thrust on the yaw and pitch respectively. A dynamic modeling has been carried out and an optimal control of a TRMS is discussed in S.M.Ahmad et al. (2000). As the rotor speeds are varying, high amount of cross coupling creeps into the system which no longer keeps the system flat, in other words, the states and input cannot be reconstructed from the output and their derivative. Controllers are designed in Mullhaupt et al. (1997, 1999); P. Mullhaupt and Bonvin (2008) by approximating the system to be a flat one. In Lu and Wen (2007), the twin rotor system is decoupled into two SISO systems with coupling effects considered as disturbances. Separate controllers have been designed for both the decoupled systems and combined. An adaptive control approach based on the backstepping concept is presented in Yang and Kim (1999) to stabilize the TRMS.

The main contribution of this paper is the design and experimental validation of terminal sliding mode control to stabilize the linearized dynamics of the TRMS about the hovering position.

The paper is organized as follows. Section II describes the modeling of TRMS based on Lagrangian approach.

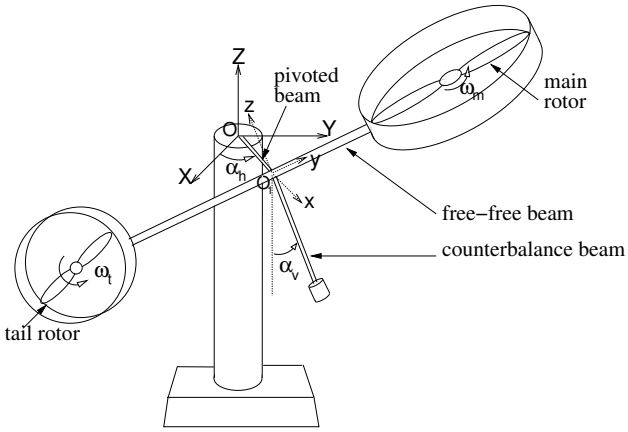


Fig. 1. Schematic of twin rotor MIMO setup

Linearization of the nonlinear model and its analysis is presented in section III. In section IV we present the terminal sliding mode control of TRMS that stabilizes the system about an operating point. The implementation results are presented in section V and the conclusion remarks are made in section VI.

## 2. MODEL

The dynamic model of the TRMS, was first derived in Rahideh and Shaheed (2007) using Lagrangian based formulation of equations of motion. For the sake of completeness, the model is re-derived. Denote by $\alpha_v$ the angle subtended by the counterbalance beam with the vertical in the anticlockwise direction, and by $\alpha_h$ the angle subtended by the pivoted beam with the X-axis as shown in Figure 1. Let $\omega_m$ be the angular velocity of the main rotor and $\omega_r$ be the angular velocity of the tail rotor. The twin rotor is a multi-body system consisting of the free-free beam (the main and the tail beam), the counterbalance beam, the pivoted beam, the main rotor and the tail rotor. Please refer to Table 1 where the system parameters are defined with their numerical values for the laboratory setup. Let

$XYZ$ be the inertial coordinate frame attached to the rotational joint of the twin rotor with the origin at $O$. Further, $xyz$ be the body-coordinate frame of the free-free beam with the origin at $O_1$. Then $\alpha_v$ and $\alpha_h$ represent the angular positions of the free-free beam about the $x$ and $z$ axes. The corresponding rotation matrices are

$$R_z = \begin{bmatrix} \cos\alpha_h & -\sin\alpha_h & 0 \\ \sin\alpha_h & \cos\alpha_h & 0 \\ 0 & 0 & 1 \end{bmatrix}; R_x = \begin{bmatrix} 1 & 0 & 0 \\ 0 & \cos\alpha_v & -\sin\alpha_v \\ 0 & \sin\alpha_v & \cos\alpha_v \end{bmatrix}.$$

The composition $R \triangleq R_z(\alpha_h)R_x(\alpha_v)$ yields the net orientation of the body frame $xyz$ with respect to the inertial frame $XYZ$. The rotation matrix is

$$R = \begin{bmatrix} \cos\alpha_h & -\sin\alpha_h\cos\alpha_v & \sin\alpha_h\sin\alpha_v \\ \sin\alpha_h & \cos\alpha_h\cos\alpha_v & -\cos\alpha_h\sin\alpha_v \\ 0 & \sin\alpha_v & \cos\alpha_v \end{bmatrix}.$$

For convenience, we write the energy equations of each of the rigid body that constitutes the twin rotor system.

*Free-free beam*

The kinetic energy associated with the free-free beam is given by

$$T_1 = \frac{J_1}{2}[(\dot\alpha_h^2\cos^2\alpha_v + \dot\alpha_v^2] + \frac{1}{2}m_{T1}h^2\dot\alpha_h^2 - m_{T1}l_{T1}h\dot\alpha_v\dot\alpha_h\sin\alpha_v$$

while its potential energy is $V_1 = m_{T1}gl_{T1}\sin\alpha_v$ , where

$$\begin{aligned} J_1 &= \frac{1}{3}m_t l_t^2 + m_{tr}l_t^2 + m_{ts}l_t^2 + \frac{1}{3}m_m l_m^2 + m_{mr}l_m^2 \\ &\quad + m_{ms}l_m^2 + \frac{1}{2}m_{ms}r_{ms}^2 + m_{ts}r_{ts}^2 \\ m_{T1} &= m_t + m_{tr} + m_{ts} + m_m + m_{mr} + m_{ms} \\ l_{T1} &= \frac{(m_m/2 + m_{mr} + m_{ms})l_m}{m_{T1}} \\ &\quad - \frac{(m_t/2 + m_{tr} + m_{ts})l_t}{m_{T1}}. \end{aligned}$$

*Counterbalance beam*

The kinetic energy associated with the counter-balance beam is given by

$$T_2 = \frac{J_2}{2}[\dot\alpha_h^2\sin^2\alpha_v + \dot\alpha_v^2] + \frac{1}{2}m_{T2}h^2\dot\alpha_h^2 + m_{T2}l_{T2}h\dot\alpha_v\dot\alpha_h\cos\alpha_v$$

while its potential energy is $V_2 = -m_{T2}gl_{T2}\cos\alpha_v$ , where

$$\begin{aligned} J_2 &= \frac{1}{3}m_b l_b^2 + m_{cb}l_{cb}^2 \\ m_{T2} &= m_b + m_{cb} \\ l_{T2} &= \frac{m_b l_b/2 + m_{cb}l_{cb}}{m_{T2}}. \end{aligned}$$

*Pivoted beam*

The kinetic energy associated with the pivot beam is $T_3 = \frac{J_3}{2}(\dot\alpha_h)^2$ where, $J_3 = \frac{m_b h^2}{3}$ and it does not contribute to the total potential energy.

*Kinetic energy of rotors*

Finally, the rotational kinetic energies associated with the main rotor and the tail rotor are

$$\begin{aligned} T_4 &= \frac{1}{2}J_{mr}[(e_3^\top)(R^{-1}\dot R)^\vee + \omega_m]^2 \\ &= \frac{1}{2}J_{mr}[\dot\alpha_h\cos\alpha_v + \omega_m]^2 \\ T_5 &= \frac{1}{2}J_{tr}[(e_1^\top)(R^{-1}\dot R)^\vee + \omega_r]^2 = \frac{1}{2}J_{tr}[\dot\alpha_v + \omega_r]^2 \end{aligned}$$

where,

$$\begin{aligned} J_{mr} &= J_{mm} + J_{m,prop} \\ J_{tr} &= J_{mm} + J_{t,prop} \end{aligned}$$

$J_{mm}$ being the moment-of-inertia of the motors about their axis of rotation, $J_{m,prop}$ and $J_{t,prop}$ are the moments-of-inertia of the main and tail rotor propellers, and $e_i$'s are the standard basis vectors in $\mathbb{R}^3$. The matrix $R^{-1}\dot R$ is skew-symmetric matrix and for a skew-symmetric matrix

$$S = \begin{bmatrix} 0 & -a & b \\ a & 0 & -c \\ -b & c & 0 \end{bmatrix}$$

the vector $S^\vee$ is defined as $S^\vee = [a\ b\ c]^\top$. The vector

$$(R^{-1}\dot R)^\vee = \begin{bmatrix} \dot\alpha_v \\ \dot\alpha_h\sin(\alpha_v) \\ \dot\alpha_h\cos\alpha_v \end{bmatrix}$$

corresponds to the angular velocity components in the body coordinate frame.

*Euler-Lagrangian equations of motion*

The Lagrangian $\mathcal{L}(\alpha_v, \alpha_h, \dot\alpha_v, \dot\alpha_h, \omega_m, \omega_r)$, defined as the difference between the total kinetic ($\sum_{i=1}^5 T_i$) and total potential energy ($V_1 + V_2$) is given by

$$\begin{aligned} \mathcal{L} &= \frac{1}{2}\{a_1\dot\alpha_v^2 + \dot\alpha_h^2(a_5 + a_4\cos^2\alpha_v) + a_6\omega_r^2 + a_7\omega_m^2 \\ &\quad + \dot\alpha_v\dot\alpha_h(a_2\cos\alpha_v - a_3\sin\alpha_v) + a_6\omega_r\dot\alpha_v \\ &\quad + a_7\omega_m\dot\alpha_h\cos\alpha_v - b_1\sin\alpha_v + b_2\cos\alpha_v. \end{aligned}$$

The corresponding Euler-Lagrange equations of motion are

$$D(\alpha_v)\begin{bmatrix} \ddot\alpha_v \\ \ddot\alpha_h \\ \dot\omega_m \\ \dot\omega_r \end{bmatrix} + \Phi(\alpha_v, \alpha_h, \dot\alpha_v, \dot\alpha_h, \omega_m, \omega_r) = F_{ext} \quad (1)$$

where, the inertia matrix $D(\alpha_v) \in \mathbb{R}^{3\times 3}$ is

$$\begin{bmatrix} a_1 & a_2\cos\alpha_v - a_3\sin\alpha_v & 0 & a_6 \\ a_2\cos\alpha_v - a_3\sin\alpha_v & a_5 + a_4\cos^2\alpha_v & a_7\cos\alpha_v & 0 \\ 0 & a_7\cos\alpha_v & a_7 & 0 \\ a_6 & 0 & 0 & a_6 \end{bmatrix}$$

and the vector of Coriolis and centrifugal forces is

$$\Phi = \begin{bmatrix} \sin\alpha_v(a_4\dot\alpha_h^2\cos\alpha_v + a_7\omega_m\dot\alpha_h + b_2) + b_1\cos\alpha_v \\ \dot\alpha_v\sin\alpha_v(-2a_4\dot\alpha_h\cos\alpha_v - a_2\dot\alpha_v - a_7\omega_m) - a_3\dot\alpha_v^2\cos\alpha_v \\ -a_7\dot\alpha_h\dot\alpha_v\sin\alpha_v \\ 0 \end{bmatrix}.$$

The constants $a_i, i = 1, \ldots, 7$ are defined as

$$\begin{aligned} &a_1 = J_1 + J_2 + J_{tr}; && a_2 = hm_{T2}l_{T2} \\ &a_3 = hm_{T1}l_{T1}; && a_4 = J_1 + J_{mr} - J_2 \\ &a_5 = m_{T1}h^2 + m_{T2}h^2 + J_3 + J_2; && a_6 = J_{tr} \\ &a_7 = J_{mr}; && b_1 = m_{T1}l_{T1}g \\ &b_2 = m_{T2}l_{T2}g; \end{aligned}$$

The various external forces that influence the dynamics of the twin rotor system are:

(1) The external forces which influence the pitch angle ($\alpha_v$) are: the aerodynamic thrust force generated by the main rotor propeller ($F_m = k_{fv}\omega_m|\omega_m|$) - the drag torque due to air friction on the tail rotor propeller ($T_r = k_{tr}\omega_r|\omega_r|$)- viscous friction force ($f_{rv}\dot{\alpha}_v$).
(2) The external forces which influence the yaw ($\alpha_h$) are: the aerodynamic force due to tail rotor propeller ($F_r = k_{fh}\omega_r|\omega_r|$)- the drag torque on the main rotor propeller ($T_m = k_{tm}\omega_m|\omega_m|$)- viscous friction force ($f_{rh}\dot{\alpha}_h$).
(3) The forces which influence the main rotor rotation are: the torque produced by motor ($\tau_m$)- drag (air friction) on the propeller ($k_{tm}\omega_m|\omega_m|$)- friction ($B_{mr}\omega_m$).
(4) The forces which influence the tail rotor rotation are: the torque produced by motor ($\tau_r$)- drag (air friction) on the propeller ($k_{tr}\omega_r|\omega_r|$)- friction ($B_{tr}\omega_r$).

Hence the vector of external forces can be written as

$$F_{ext} = \begin{bmatrix} l_m k_{fv}\omega_m|\omega_m| - k_{tr}\omega_r|\omega_r| - f_{rv}\dot{\alpha}_v \\ l_t k_{fh}\omega_r|\omega_r|\cos\alpha_v - k_{tm}\omega_m|\omega_m|\cos\alpha_v - f_{rh}\dot{\alpha}_h \\ \tau_m - k_{tm}\omega_m|\omega_m| - B_{mr}\omega_m \\ \tau_r - k_{tr}\omega_r|\omega_r| - B_{tr}\omega_r. \end{bmatrix}$$

*State-space formulation*

The dynamics of the system is expressed in the state-space form by choosing the state variables as $x = (x_1, x_2, x_3, x_4, x_5, x_6) \triangleq (\alpha_v, \alpha_h, \dot{\alpha}_v, \dot{\alpha}_h, \omega_m, \omega_r)$. The resulting sixth-order state-space model is given by

$$\dot{x} = f(x) + g_1(x)\tau_m + g_2(x)\tau_r \tag{2}$$

where, $f(x) = [x_3 \;\; x_4 \;\; \beta_1(x) \;\; \beta_2(x) \;\; \beta_3(x) \;\; \beta_4(x)]^\top$, $g_1(x) = [0 \;\; 0 \;\; \lambda_1(x) \;\; \lambda_2(x) \;\; \lambda_3(x) \;\; \lambda_4(x)]^\top$ and $g_2(x) = [0 \;\; 0 \;\; \delta_1(x) \;\; \delta_2(x) \;\; \delta_3(x) \;\; \delta_4(x)]^\top$. The components $\beta_i, \gamma_i, \delta_i$, $i = 1, \ldots, 4$ of the drift and control vectors are given by

$$\begin{aligned} \beta_i \;=\; & x_4^2\left(-a_4 n_{i1}\cos x_1 \sin x_1\right) + x_3^2(a_2 n_{i2}\sin x_1 \\ & + a_3 n_{i2}\cos x_1) \\ & + x_3 x_4\left(2a_4 n_{i2}\cos x_1 \sin x_1 + a_7 n_{i3}\sin x_1\right) \\ & + x_4 x_5\left(-a_7 n_{i1}\sin x_1\right) + x_3 x_5\left(a_7 n_{i2}\sin x_1\right) \\ & + x_5|x_5|\left(l_m k_{fv} n_{i1} - k_{tm} n_{i2}\cos x_1 - n_{i3} k_{tm}\right) \\ & + x_6|x_6|\left(l_t k_{fh} n_{i2}\cos x_1 - k_{tr} n_{i1} - n_{i4} k_{tr}\right) \\ & + x_3\left(-n_{i1} f_{rv}\right) + x_4\left(-n_{i2} f_{rh}\right) + x_5\left(-B_{mr} n_{i3}\right) \\ & + x_6\left(-B_{tr} n_{i4}\right) + b_1\left(-n_{i1}\cos x_1\right) - b_2\left(n_{i1}\sin x_1\right) \\ \lambda_i \;=\; & n_{i3} \\ \delta_i \;=\; & n_{i4}. \end{aligned}$$

where the terms $n_{ij}$ are the elements of $D(\alpha_v)^{-1}$. If $h$, the beam offset is set to zero in (1), we recover the model presented in P. Mullhaupt and Bonvin (2008), except for the static friction term that is neglected in this paper. The friction coefficients $f_{rv}$ and $f_{rh}$ are ignored as the effect of friction is negligible.

## 3. LINEARIZATION AND ANALYSIS OF ZERO DYNAMICS

In this section, we linearize the state-space model about an operating point, in order to study the local behaviour of the system. We also analyze the residual dynamics of the rotor velocities when the pitch and yaw are regulated to zero, to illustrate the non-minimum phase property of the TRMS system.

Table 1. System parameters

| | | |
|---|---|---|
| Mass of the main DC-motor with main rotor | $m_{mr}$ | 0.405 kg |
| Mass of the beam from the center towards main rotor | $m_m$ | 0.014 kg |
| Mass of the tail DC-motor with tail rotor | $m_{tr}$ | 0.36 kg |
| Mass of the beam from the center towards tail rotor | $m_t$ | 0.016 kg |
| Mass of the counterweight | $m_{cb}$ | 0.068 kg |
| Mass of the counterweight beam | $m_b$ | 0.022 kg |
| Mass of the main shield | $m_{ms}$ | 0.165 kg |
| Mass of the tail shield | $m_{ts}$ | 0.095 kg |
| Length of the beam from the center to main rotor | $l_m$ | 0.246 m |
| Length of the beam from the center towards tail rotor | $l_t$ | 0.282 m |
| Length of the counterweight beam | $l_b$ | 0.25 m |
| Distance between counterweight and joint | $l_{cb}$ | 0.24 m |
| Length of the offset between base and joint | $h$ | $6 \times 10^{-2}$ m |
| Radius of the main rotor shield | $r_{ms}$ | 0.155 m |
| Radius of the tail rotor shield | $r_{ts}$ | 0.1 m |
| Acceleration due to gravity | $g$ | 9.81 m/s$^2$ |
| Moment-of-inertia of main rotor | $J_{mr}$ | $2 \times 10^{-4}$ kg m$^2$ |
| Moment-of-inertia of tail rotor | $J_{tr}$ | $2.6 \times 10^{-5}$ kg m$^2$ |
| Coefficient of thrust due to main rotor | $k_{fv}$ | $1.13 \times 10^{-5}$ kgm |
| Coefficient of thrust due to tail rotor | $k_{fh}$ | $2.23 \times 10^{-6}$ kgm |
| Main motor friction coefficient | $B_{mr}$ | $2.0972 \times 10^{-5}$ kg m$^2$/s |
| Tail motor friction coefficient | $B_{tr}$ | $1.1817 \times 10^{-5}$ kg m$^2$/s |
| Main rotor drag coefficient | $k_{tm}$ | $3.6457 \times 10^{-7}$ kg m$^2$ |
| Tail rotor drag coefficient | $k_{tr}$ | $2.436 \times 10^{-8}$ kg m$^2$ |

The hovering position of the TRMS is the position of interest. The operating point is $x^* = (0, 0, 0, 0, \omega_m^*, \omega_r^*)$, where $\omega_m^*$ and $\omega_r^*$ are the velocities of the main rotor and tail rotor respectively to keep the TRMS in the hovering position. With $\alpha_v = \alpha_h = 0$, $\omega_m = \omega_m^*$ and $\omega_r = \omega_r^*$, and the derivatives $\dot{\alpha}_v = \dot{\alpha}_h = \ddot{\alpha}_v = \ddot{\alpha}_h = \dot{\omega}_m = \dot{\omega}_r = 0$, (2) reduces to

$$\begin{aligned} l_m k_{fv}\omega_m|\omega_m| - k_{tr}\omega_r|\omega_r| &= b_1 \\ l_t k_{fh}\omega_r|\omega_r| - k_{tm}\omega_m|\omega_m| &= 0 \\ \tau_m - B_{mr}\omega_m - k_{tm}\omega_m|\omega_m| &= 0 \\ \tau_r - B_{tr}\omega_r - k_{tr}\omega_r|\omega_r| &= 0. \end{aligned}$$

Hence the rotor velocities at the given operating point are

$$\omega_m^* = \sqrt{\frac{b_1 l_t k_{fh}}{l_m k_{fv} l_t k_{fh} - k_{tr} k_{tm}}}$$

$$\omega_r^* = \sqrt{\frac{b_1 k_{tm}}{l_m k_{fv} l_t k_{fh} - k_{tr} k_{tm}}}$$

and the corresponding motor torques are

$$\tau_m^* = k_{tm}\omega_m^*|\omega_m^*| + B_{mr}\omega_m^*$$
$$\tau_r^* = k_{tr}\omega_t^*|\omega_t^*| + B_{tr}\omega_t^*.$$

The state-space model given by (2) is linearized about the operating point $x^* = (0, 0, 0, 0, \omega_m^*, \omega_r^*)$, yielding

$$\dot{z} = Az + Bv \tag{3}$$

where,

$$z \triangleq x - x^*$$
$$v \triangleq \begin{bmatrix} \tau_m - \tau_m^* \\ \tau_r - \tau_r^* \end{bmatrix}$$
$$A \triangleq \left.\frac{\partial f}{\partial x}\right|_{x=x^*} + \tau_m^* \left.\frac{\partial g_1}{\partial x}\right|_{x=x^*} + \tau_r^* \left.\frac{\partial g_2}{\partial x}\right|_{x=x^*}$$
$$B \triangleq \left.[g_1(x)\ g_2(x)]\right|_{x=x^*}.$$

Using the constants from Table 1, the numerical values for the A and B matrices are:

$$A = \begin{bmatrix} 0 & 0 & 1 & 0 & 0 & 0 \\ 0 & 0 & 0 & 1 & 0 & 0 \\ -2.3778 & 0 & 0 & 0 & 0.01419 & 0.00011 \\ 0.03468 & 0 & 0 & 0 & 0.00006 & 0.00245 \\ -0.03468 & 0 & 0 & 0 & -0.8372 & -0.00245 \\ 2.3778 & 0 & 0 & 0 & -0.01419 & -0.7412 \end{bmatrix};$$

$$B = \begin{bmatrix} 0 & 0 \\ 0 & 0 \\ 0.1854 & -12.7106 \\ -12.7106 & 0.1854 \\ 5.0128 \times 10^3 & 0.202 \\ 0.202 & 3.8474 \times 10^4 \end{bmatrix}.$$

The open-loop eigen values for the linearized system (3) are $\lambda(A) = (0, 0, 4.065 \times 10^{-5} \pm i1.5420, -0.7410, -0.8375)$. The zero eigen values correspond to the state $x_2 = \alpha_h$, as the system dynamics are invariant with respect to $\alpha_h$. The eigen space corresponding to the eigen value 0 is one-dimensional, meaning that $A$ is not diagonalizable. Also, the system has two eigen values with positive real parts, rendering the origin of (3) unstable. For the linearized model of the TRMS given by (3), the controllable matrix has rank six and hence is completely controllable.

### *3.1 Zero dynamics (Non-minimum phase property)*

The zero dynamics of a system are those residual dynamics remaining after the outputs have been regulated to identically zero values. A nonlinear system is said to be non-minimum phase when its zero dynamics are unstable. In P. Mullhaupt and Bonvin (2008), it was shown that the toycopter had unstable zero dynamics with the outputs being the pitch and yaw angles. A similar result will be shown here for the TRMS. Unstable zero dynamics with these natural outputs implies that an output regulation type of control will render the system unstable. For feedback linearizable systems, we can always find a set of outputs such that there are no residual dynamics remaining. However, for systems which are not fully feedback linearizable, the residual dynamics are non-trivial.

The notion of relative degree, as defined in Isidori (1995), is helpful in understanding the zero dynamics of a system. Since the TRMS is a MIMO system, we consider the vector relative degree, also defined in Isidori (1995). The term, vector relative degree relates to the number of times the outputs are to be differentiated to explicitly obtain the inputs. Consider the nonlinear state-space model of the TRMS given by (2). If the outputs are chosen to be $y_1 = \alpha_v$ and $y_2 = \alpha_h$, then the vector relative degree is $[2\ 2]^\top$, defined at all points in the state-space.

If the outputs are considered to be $y_1 = x_1$ and $y_2 = x_2$ and if $y_1 \equiv y_2 \equiv 0$, then the residual dynamics are

$$a_6\dot{\omega}_r = l_m k_{fv}\omega_m|\omega_m| - k_{tr}\omega_r|\omega_r| - b_1$$
$$a_7\dot{\omega}_m = l_t k_{fh}\omega_r|\omega_r| - k_{tm}\omega_m|\omega_m|.$$

These zero dynamics have the equilibrium point $(\omega_m, \omega_r) = (\omega_m^*, \omega_r^*)$. Linearizing about the equilibrium point, we obtain

$$\begin{bmatrix} \delta\dot{\omega}_m \\ \delta\dot{\omega}_r \end{bmatrix} = \begin{bmatrix} -\dfrac{2k_{tm}\omega_m^*}{a_7} & \dfrac{2l_t k_{fh}\omega_r^*}{a_7} \\ \dfrac{2l_m k_{fv}\omega_m^*}{a_6} & -\dfrac{2k_{tr}\omega_r^*}{a_6} \end{bmatrix} \begin{bmatrix} \delta\omega_m \\ \delta\omega_r \end{bmatrix}. \tag{4}$$

The eigen values of the linearized dynamics (4) are expressed as

$$\lambda_{1,2} = -\frac{k_{tm}\omega_m^*}{a_7} - \frac{k_{tr}\omega_r^*}{a_6} \pm \sqrt{\left(\frac{k_{tm}\omega_m^*}{a_7} - \frac{k_{tr}\omega_r^*}{a_6}\right)^2 + 4\frac{l_t k_{fh} l_m k_{fv}\omega_m^*\omega_r^*}{a_6 a_7}}. \tag{5}$$

The drag coefficients $k_{tm}$ and $k_{tr}$ are about an order of magnitude lesser than the thrust coefficients $l_m k_{fv}$ and $l_t k_{fh}$, and therefore the second term in (5) is always larger than the first. Hence, the equilibrium point $(\omega_m, \omega_r)$ of linearized dynamics (4) is a saddle point. Therefore, the zero dynamics of the TRMS is unstable. In particular, for the constants specified in Table 1, the eigen values of the zero dynamics are $(-6.9409, 5.9219)$.

## 4. THIRD-ORDER SLIDING MODE CONTROL FOR THE TRMS

Sliding mode is one of the robust controller design method and it has been successfully applied to many practical systems. It has been applied to several nonholonomic mechanical systems in the works of Edwards and Spurgeon (1998); Riachy et al. (2008); Utkin et al. (2009); Yang and Kim (1999). In Venkataraman and Gulati (1993), the authors introduced the notion of terminal sliding mode wherein the control law is such that it results in finite time convergence of the state trajectory, unlike in conventional sliding mode control. The advantage that terminal sliders provide is the robustness to parametric uncertainty without having to resort to high frequency control switching. In the previous section we saw that the system has unstable zero dynamics for the outputs $y_1 = x_1$ and $y_2 = x_2$. This rules out using first-order sliding mode control with sliding functions of the form $\phi(x_1, x_2, x_3, x_4)$, as well as second-order sliding mode control with sliding functions of the form $\psi(x_1, x_2)$ as the zero dynamics associated with $y = [x_1\ \ x_2]^\top$ is unstable. Although there may be other first-order or second-order sliding functions which also include $x_5$ and $x_6$, it is difficult to analyze the residual dynamics. If there exist two nonlinear sliding functions which have relative degrees $r_1$ and $r_2$ such that $r_1 + r_2 = 6$, then the residual dynamics are restricted to the origin and the corresponding control law results in

finite time convergence. But the existence of such functions is not guaranteed. In fact, if the TRMS is not feedback linearizable, we cannot find a pair of functions such that there are no residual dynamics. However, the system is linearly controllable, and the linear approximation made in (3) holds over a fairly wide range about the operating point.

The nonlinear system may have a maximal vector relative degree of [2 2], but since it is linearly controllable at the desired operating point, the linearized system is finite time stabilizable as shown in Hong (2002). Consider the linearized system given by equation (3). We choose a pair of vectors $C_1$ and $C_2$ such that

$$C_1^\top B = C_2^\top B = 0$$
$$C_1^\top AB = C_2^\top AB = 0.$$

Equivalently, we can write $C_1, C_2 \in \mathcal{N}_l([B\ AB])$ where $\mathcal{N}_l(P)$ stands for the left null space of the matrix $P$. The columns of $[B\ AB]$ are linearly independent for the linearized model. Hence, this matrix has a two-dimensional left null space. This allows us to choose two linearly independent vectors $C_1$ and $C_2$. Then, we define the sliding functions as

$$s_1 = C_1^\top z$$
$$s_2 = C_2^\top z.$$

This choice leads to the derivatives of $s_1, s_2$ as

$$\dot{s}_1 = C_1^\top Az \qquad \dot{s}_2 = C_2^\top Az$$
$$\ddot{s}_1 = C_1^\top A^2 z \qquad \ddot{s}_2 = C_2^\top A^2 z.$$

Thus, the inputs do not appear until the third derivative of $s_1$ and $s_2$. The inputs can be derived from

$$s_1^{(3)} = C_1^\top A^3 z + C_1^\top A^2 Bv$$
$$s_2^{(3)} = C_2^\top A^3 z + C_2^\top A^2 Bv.$$

Denoting $C = \begin{bmatrix} C_1^\top \\ C_2^\top \end{bmatrix}$, the control law is

$$v = (CA^2B)^{-1}CA^3 z + \begin{bmatrix} v_{ft,1} \\ v_{ft,2} \end{bmatrix}. \tag{6}$$

The matrix $CA^2B$ is invertible since the system (3) is controllable, and $C_1$ and $C_2$ are independent non-zero vectors in the left null space of $[B\ AB]$. The variables $v_{eq,1}$ and $v_{eq,2}$ are the equivalent control inputs, and take on zero value on the sliding surface. The functions $v_{ft,1}$ and $v_{ft,2}$ represent inputs which stabilize the origin of the two-input triple integrator system

$$\begin{aligned} \dot{\xi}_1 &= \xi_2 & \dot{\xi}_4 &= \xi_5 \\ \dot{\xi}_2 &= \xi_3 & \dot{\xi}_5 &= \xi_6 \\ \dot{\xi}_3 &= v_{ft,1} & \dot{\xi}_6 &= v_{ft,2} \end{aligned} \tag{7}$$

in finite time. The system (7) represents the Brunovsky canonical form of (3) and it can be transformed to the form (7) by choosing $\xi_1 = s_1$, $\xi_2 = \dot{s}_1$, $\xi_3 = \ddot{s}_1$, $\xi_4 = s_2$, $\xi_5 = \dot{s}_2$ and $\xi_6 = \ddot{s}_2$. There are no residual dynamics for the linearized system since $r_1 + r_2 = 6 = n$. Hence (6) represents a terminal-sliding mode control for the linearized system (3). A finite-time stabilizing control law is chosen based on the procedure outlined in Hong (2002), which gives us a continuous control law. In particular, to stabilize the system (7), we use the finite-time control laws:

$$\begin{aligned} v_{ft,1} &= -l_{31}\left[l_{21}\left(x_1^5 + x_2^{45/7}\right)^{1/9} + x_3\right]^{3/5} \\ v_{ft,2} &= -l_{32}\left[l_{22}\left(x_1^5 + x_2^{45/7}\right)^{1/9} + x_3\right]^{3/5} \end{aligned} \tag{8}$$

The constants $l_{21}$, $l_{22}$, $l_{31}$ and $l_{32}$ can be chosen based on the procedure outlined in Hong (2002). Since only lower bounds are specified, we can ensure stability by choosing a high value for these constants. Since this is terminal sliding mode control, we only need to prove stability for the reaching phase. Controllable multi-input linear systems are shown to be finite-time stabilizable in Hong (2002). The system represented by (7) is also shown to be finite time stable with the control law (8). Although sliding mode control is robust to parametric uncertainties, it is difficult to perform a robustness analysis in this case, since variations in many parameters cause the operating point itself to shift.

## 5. EXPERIMENTAL RESULTS

The third-order sliding mode control is defined as in (6) with the vectors $C_1$ and $C_2$ obtained from the left null space of $[B\ AB]$. For the parameter values presented in Table 1, we use the following vectors, which form an orthonormal basis for the left null space (obtained using singular value decomposition):

$$C_1 = \begin{bmatrix} -0.9908 \\ 2.813 \times 10^{-3} \\ -0.0165 \\ -0.1344 \\ -3.414 \times 10^{-4} \\ -4.792 \times 10^{-6} \end{bmatrix},\ C_2 = \begin{bmatrix} 1.156 \times 10^{-3} \\ -0.9841 \\ -0.1773 \\ -7.346 \times 10^{-3} \\ -1.206 \times 10^{-5} \\ -5.849 \times 10^{-5} \end{bmatrix}$$

With this choice of $C_1$ and $C_2$, the matrix $CA^2B$ is given by

$$CA^2B = \begin{bmatrix} -70.57 & 4.8011 \\ 10.3827 & -98.1095 \end{bmatrix}$$

and is invertible. The values of the constants for the finite time control law (8) are chosen as

$$l_{21} = 1.6,\ l_{22} = 1.2,\ l_{31} = 6,\ l_{32} = 8.$$

The third-order sliding mode control is implemented on the TRMS setup developed by Feedback$^{\text{TM}}$ Instruments Limited using Simulink$^{\text{TM}}$. Encoders are used to measure the angular positions of the pitch $x_1$ and yaw $x_2$. We note that the range of pitch and yaw angles are restricted to the interval $(-\pi/2, \pi/2)$ due to the physical limits on the setup. Tachometers are used to measure the rotor angular velocities $x_5$ and $x_6$. The pitch and yaw velocity information is obtained by differentiating the corresponding position information.

A torque to voltage conversion is performed for both motors, which does an approximate inversion of the motor model utilizing the rotor angular velocities. As reported in Rahideh and Shaheed (2007), the relationship between the applied voltage to the DAC via Simulink and the actual voltage at the motor terminals is nonlinear. Hence, a lookup table is generated for this relationship and the voltages obtained through the lookup table are fed to the DAC.

Since the dynamics is invariant with respect to the yaw, and the encoders assume the initial position to be zero,

different initial conditions for the yaw can be given by starting it at the default position and specifying different final positions. However, the flat cable used for connecting the sensors to the main unit exerts a torque on the system if the yaw is not at the default position, and thus may cause a slight error in the position.

To validate the performance of the controller, experiments were conducted to obtain the response of the system to the disturbances in the pitch (see Figure 2) and disturbances in the yaw (see Figure 3).

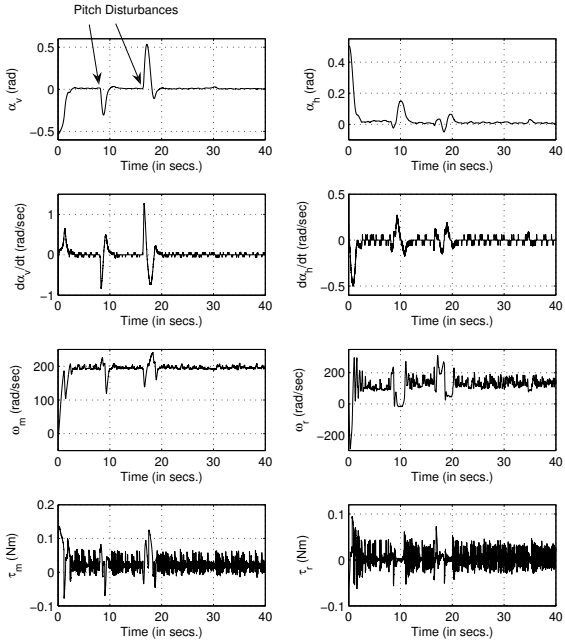


Fig. 2. Experimental results: States and inputs with pitch disturbances

## 6. CONCLUSIONS

In this paper a terminal sliding mode controller is presented to stabilize the linearized model of the TRMS about the hovering position. Experimental results clearly validate the efficacy of the controller over a large domain about the operating point. Further the sliding mode controller responds quickly in attenuating the disturbances.

## REFERENCES

Edwards, C. and Spurgeon, S.K. (1998). *Sliding Mode Control*. Taylor and Francis, London.

Hong, Y. (2002). Finite-time stabilization and stabilizability of a class of controllable systems. *Systems and Control Letters*, 46, 231–236.

Isidori, A. (1995). *Nonlinear Control Systems*. Spinger Verlag, New York.

Lu, T.W. and Wen, P. (2007). Time optimal and robust control of twin rotor system. In *IEEE International Conference on Control and Automation*, 862–866. Guangzhou, China.

Mullhaupt, P., Srinivasan, B., Lévine, J., and Bonvin, D. (1997). Modelling and control of a twin rotor multi-input multi-output system. In *Proceedings of the European Control Conference*, 431–435. Brussels, Belgium.

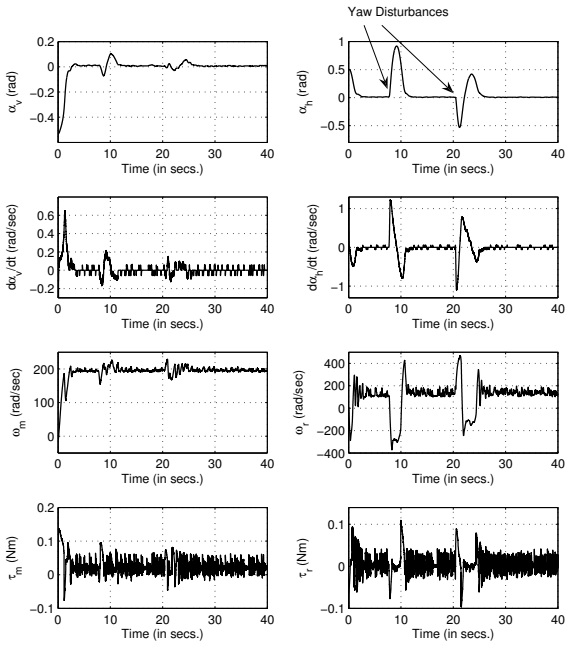


Fig. 3. Experimental results: States and inputs with yaw disturbances

Mullhaupt, P., Srinivasan, B., Lévine, J., and Bonvin, D. (1999). Cascade control of the toycopter. In *European Control Conference*, 1010–1012. Karlsruhe, Germany.

P. Mullhaupt, B. Srinivasan, J.L. and Bonvin, D. (2008). Control of the toycopter using a flat approximation. *Transactions on Control System Technology*, 16(5), 882–896.

Rahideh, A. and Shaheed, M. (2007). Mathematical dynamic modelling of a twin-rotor multiple inputmultiple output system. *Proc. IMechE Part I: J. Systems and Control Engineering*, 221, 89–101.

Riachy, S., Orlov, Y., Floquet, T., Santiesteban, R., and Richard, J.P. (2008). Second-order sliding mode control of underactuated mechanical systems ı: Local stabilization with application to an inverted pendulum. *International Journal of Robust and Nonlinear Control*, 18(4-5), 529–543.

S.M.Ahmad, A.J.Chipperfield, and M.O.Tokhi (2000). Modelling and control of a twin rotor multi-input multi-output system. In *Proceedings of the American Control Conference*, 1720–1724. Chicago, USA.

Utkin, V., Guldner, J., and Shi, J. (2009). *Sliding Mode Control in Electro-Mechanical Systems*. CRC Press, Taylor and Francis Group.

Venkataraman, S.T. and Gulati, S. (1993). Control of Nonlinear Systems Using Terminal Sliding Modes. *ASME Journal of Dynamic Systems, Measurements and Control*, 115(3), 554–560.

Yang, J.M. and Kim, J.H. (1999). Sliding-mode control for trajectory tracking of nonholonomic wheeled mobile robots. *IEEE Trans. on Robotics & Automation*, 15, 578–587.